

La Salle University

## La Salle University Digital Commons

---

HON499 projects

Honors Program

---

Fall 11-23-2021

### Barite co-precipitation of arsenic and chromium anions for the treatment of fracking wastewater

Kendra C. Schlitzer

*La Salle University*, [schlitzerk1@lasalle.edu](mailto:schlitzerk1@lasalle.edu)

Amber L. O'Connor

*La Salle University*, [oconnora3@student.lasalle.edu](mailto:oconnora3@student.lasalle.edu)

Florence T. Ling

*La Salle University*, [ling@lasalle.edu](mailto:ling@lasalle.edu)

Follow this and additional works at: [https://digitalcommons.lasalle.edu/honors\\_projects](https://digitalcommons.lasalle.edu/honors_projects)



Part of the [Environmental Studies Commons](#)

---

#### Recommended Citation

Schlitzer, Kendra C.; O'Connor, Amber L.; and Ling, Florence T., "Barite co-precipitation of arsenic and chromium anions for the treatment of fracking wastewater" (2021). *HON499 projects*. 42.

[https://digitalcommons.lasalle.edu/honors\\_projects/42](https://digitalcommons.lasalle.edu/honors_projects/42)

This Honors Project is brought to you for free and open access by the Honors Program at La Salle University Digital Commons. It has been accepted for inclusion in HON499 projects by an authorized administrator of La Salle University Digital Commons. For more information, please contact [duinkerken@lasalle.edu](mailto:duinkerken@lasalle.edu).

## **Barite co-precipitation of arsenic and chromium anions for the treatment of fracking wastewater**

KENDRA C. SCHLITZER<sup>1\*</sup>, AMBER L. O'CONNOR<sup>1</sup>, FLORENCE T. LING<sup>1</sup>

<sup>1</sup>Department of Environmental Science Program, Department of Chemistry and Biology, La Salle University, Philadelphia, PA, 19141, USA, \*schlitzerk1@lasalle.edu

Keywords: barite, arsenic, chromium, co-precipitation, fracking

### **Abstract**

Hydraulic fracturing, also known as fracking, produces wastewater that contains hazardous ions such as arsenic, strontium, and chromium. In order to remove these toxic contaminants, Na<sub>2</sub>SO<sub>4</sub> can be added to fracking wastewater to form Barite (BaSO<sub>4</sub>). During this process, ions such as Arsenic and Chromium will incorporate into the solid phase. In this work, we examined the co-precipitation of Arsenic and Chromium anions into Barite. We have created simulations of this precipitate formation in fracking wastewater treatments and have used this for Arsenic, Chromium, and Barium. A 1:1 ratio of BaCl<sub>2</sub> to Na<sub>2</sub>SO<sub>4</sub> at saturation indices of 2.19, 2.89, 3.49 for BaSO<sub>4</sub> were used for experimentation. We conducted two more experiment sets at 1.0 M NaCl to analyze the effect of salinity with the same experiment concentration and an adjusted concentration to result in identical saturation indices. Na<sub>2</sub>SO<sub>4</sub> was added to the simulated fracking wastewater. X-ray fluorescence was conducted to analyze the concentrations of Chromium, Arsenic, and Barium in precipitated solids. Fracking wastewater solutions that are undersaturated with respect to BaCrO<sub>4</sub> have undetectable levels of Chromium. For experiments that are oversaturated with respect to Barium Chromate, the Chromium concentration increases as NaCrO<sub>4</sub> (M) increases with and without NaCl. Arsenic incorporation into Barite somewhat correlates with HAsO<sub>4</sub><sup>2-</sup> but is complicated by competition with CrO<sub>4</sub><sup>2-</sup>. As BaSO<sub>4</sub> saturation index increases, Chromium incorporation decreases. Arsenic incorporation also increases with BaSO<sub>4</sub> saturation index until a threshold is reached, likely due to competition with Chromium. Increased NaCl leads to Barite particles that are more concentrated in Chromium and Arsenic. These results have implications for how competing anions are affected during the treatment of fracking wastewater using co-precipitation.

### **Introduction**

Hydraulic fracturing, also known as fracking, refers to the use of highly pressurized water to drill into the ground and produce natural gas (Lutz, et al.). The drilling occurs deep below earth's surface and involves large amounts of water, chemicals, and sand being used to break up sedimentary rock formations that block any desired natural gas. Water is sprayed at an extremely pressurized level where rock can break and release any natural gas that is being blocked by the rock formations. After drilling, the fracking fluid is pumped to the surface. The fluid that rises to the surface can include wastewater that is contaminated by the toxic chemicals in the fluid, which gets stored in either pits or disposed in wells underground (Denchak). This wastewater from fracking fluid can interact with the salts and other brines in the ground which contains

hazardous anions like arsenic, strontium, and chromium (Bamberger, et al.). Wastewater from fracking fluid that reaches the surface after the initial drilling occurs, also known as flowback water, can also contain these hazardous anions and present a hazard to humans and the environment. Fracking wastewater disposal tactics is one of many environmental concerns with fracking, as wastewater reaching outside environments can cause damage to any living or nonliving thing it comes in contact with. Fracking flowback water and produced water both contain high concentrations of Chromium and Arsenic as well as Barium, Radium, Strontium, etc. Exposure to these toxic elements can pose a risk to human and ecosystem health (Hammer). These contaminants in fracking wastewater can also enter water reservoirs and contaminate drinking water (Bamberger, et al.). Both Chromium and Arsenic are highly toxic and are classified as carcinogens for humans when consumed (Tchounwou, et al.).

Three common fracking wastewater disposal techniques are deep well injection, internal reuse and sending wastewater to a treatment plant. Deep well injection became a popular hazardous disposal tactic for different companies in the 1930's. Currently, well injection can now be applied to a broader spectrum of various hazardous wastes as well as different types of liquid wastes. The injection itself involves the storing and disposal of concentrated waste brines after desalination and internal reuse (Goodin). It allows for an underground disposal of highly concentrated waste brines post-desalination that cause a risk to human and environmental health (Zhang, et al.). It is a favored waste disposal method due to its success rates and permanence in the environment. However, some find it concerning how the injection itself is not visible to humans and could be more damaging than we may know – especially with how damaging a deep well failure can be on the environment (Goodin). Another common fracking wastewater disposal technique is internal reuse which is the reuse of collected flowback water. This is done to minimize wastewater treatment costs and other obstacles that come along with monitoring fracking wastewater (Shaffer, et al.). The option to send fracking wastewater to a treatment plant is also a common method. A handful of water treatment facilities are able to remove the salts and radioactive substances from wastewater through membrane treatment and distillation. After the wastewater is treated, the water can either be discharged into nearby surface water or used for various agricultural practices. This treatment has become popularized due to the limit and cost of other fracking wastewater disposal methods (Erikson). There are other removal techniques available but the removal of precipitated solids in wastewater with sulfate co-precipitation in treatment practices remains the most effective and environmentally conscious method (Lutz, et al.).

This initial experimental study was designed to examine the effects of solubility, salinity, saturation index and competitive ions within Barite co-precipitation. Our work in this research focuses on analyzing Chromium, Arsenic, and Barium removal from fracking wastewater. Studies have shown that Chromium and Arsenic can incorporate into the Barite ( $\text{BaSO}_4$ ) structure, although not much work has examined their competition for incorporation. Previous studies have concluded that Barite co-precipitation is most efficient when there is a high SI because of the greater chance of solid formation during co-precipitation (Rosenberg). Other studies have found that Arsenic co-precipitation in  $\text{Ba}(\text{SO}_4, \text{HAsO}_4)$  is favored when it is saturated and has high salinity; however, the reasoning for this was not understood (Ling, et al.). Therefore, we will examine the treatment of fracking contaminants using Barite formation in the water. Barium is present in fracking wastewater in high concentrations, and the addition of

Na<sub>2</sub>SO<sub>4</sub> can form BaSO<sub>4</sub>. This formation creates solid precipitation, removing trace contaminants as Barite incorporates various hazardous ions within its structure. Barite is an ideal host for this co-precipitation because it has a low solubility variable ( $K_{sp} = 10^{-9.98}$ ) which allows for a quicker formation of solid during co-precipitation and has crystals that maintain high stability in both pH ranges and temperature conditions (Tokunaga). This co-precipitation allows minor elements such as Chromium and Arsenic precipitate from solid host mineral (L'Heureux, et al.). Due to the toxicity of Chromium and Arsenic within our environment, Barite is used as a soluble mineral to initiate this removal and co-precipitation of these toxic elements. For example, Sr<sup>2+</sup>, Ca<sup>2+</sup>, and Pb<sup>2+</sup> can replace the Ba<sup>2+</sup> in BaSO<sub>4</sub> while HAsO<sub>4</sub><sup>2-</sup> and CrO<sub>4</sub><sup>2-</sup> can replace SO<sub>4</sub><sup>2-</sup> in BaSO<sub>4</sub> (Breit, et al.). That is where the work of our research participants come in as we use simulated fracking wastewater amounts to analyze the precipitated solids and come to conclusions. In this work, both Arsenic and Chromium incorporation into Barite will be examined along with the effects of NaCl. Using NaCl will allow us to analyze the effect of salinity with the same experiment concentration and an adjusted concentration to result in identical saturation indices. By comparing saturation index, we are able to compare the different difficulties in the removal process, based on saturations in the simulated wastewater solutions.

## Methods:

### Simulated Fracking Wastewater Experiments

Experiments were run by using a 1:1 ratio of BaCl<sub>2</sub> to Na<sub>2</sub>SO<sub>4</sub> at specific saturation indices (SI) of 2.19, 2.89, 3.49 for BaSO<sub>4</sub>. These saturation indices for BaSO<sub>4</sub>, which were determined earlier, are used to determine the concentrations of Ba<sup>2+</sup>, CrO<sub>4</sub><sup>2-</sup>, HAsO<sub>4</sub><sup>2-</sup> and SO<sub>4</sub><sup>2-</sup>. The following three endmember saturation indices were used to calculate the experimental ion concentrations:

$$(1) SI_{BaSO_4} = \log\left(\frac{\{Ba^{2+}\}\{SO_4^{2-}\}}{K_{sp,BaSO_4}}\right)$$

$$(2) SI_{BaCrO_4} = \log\left(\frac{\{Ba^{2+}\}\{CrO_4^{2-}\}}{K_{sp,BaCrO_4}}\right)$$

$$(3) SI_{BaHAsO_4} = \log\left(\frac{\{Ba^{2+}\}\{HAsO_4^{2-}\}}{K_{sp,BaHAsO_4}}\right)$$

We focused on HAsO<sub>4</sub><sup>2-</sup> and CrO<sub>4</sub><sup>2-</sup> co-precipitations in Barite before adding Na<sub>2</sub>SO<sub>4</sub> to a solution of BaCl<sub>2</sub>, Na<sub>2</sub>HAsO<sub>4</sub>, and Na<sub>2</sub>CrO<sub>4</sub>. Co-precipitation can occur when solid particles form into a lattice structure where a minimum stored energy can occur, which form when there is a limiting rate of reaction and a high saturation index (Noguera). When a saturation index is greater than 0, that means there is oversaturation and a greater chance for co-precipitation to occur. When the saturation index is high, this indicates the reaction being far from equilibrium, therefore, these elements can form solids in a liquid phase. In order for us to calculate the saturation indices for each endmember of the Ba(SO<sub>4</sub>, HAsO<sub>4</sub>, CrO<sub>4</sub>) system, solubility products

were used. In the Ba(SO<sub>4</sub>, HAsO<sub>4</sub>, CrO<sub>4</sub>) system, the endmembers are BaSO<sub>4</sub> (K<sub>sp</sub> = 10<sup>-9.98</sup>), BaHAsO<sub>4</sub> (10<sup>-5.6</sup>), and BaCrO<sub>4</sub> (K<sub>sp</sub> = 10<sup>-9.55681</sup>). These solubility products show that the BaSO<sub>4</sub> solubility product is the most different from the solubility product of BaHAsO<sub>4</sub>.

Two additional sets of experiments were conducted at 1.0M NaCl in order to examine the effect of salinity. One of the additional sets will have the same concentrations as the original experiments with no NaCl and the other set will have adjusted concentrations in order to keep the same 2.19, 2.89 and 3.49 saturation indices (shown in Tables 1, 2, and 3). The ion activity coefficients were calculated using the Pitzer formulation with PHREEQC software. The calculated ion activity coefficients were used to find NaCl experiments solution concentrations conducted at 2.19, 2.89 and 3.49 saturation indices of Barite. We note that Barium Arsenate had a constant saturation index while we examined Barium Chromate at lower and higher saturation indices in different experiments.

**Table 1.** Solution concentrations for the original experiments conducted without NaCl at Barite saturation indices of 2.19, 2.89, and 3.49.

Experiment	BaCl <sub>2</sub> (M)	Na <sub>2</sub> SO <sub>4</sub> (M)	Na <sub>2</sub> CrO <sub>4</sub> (M)	Na <sub>2</sub> HAsO <sub>4</sub> (M)	BaSO <sub>4</sub> SI	BaHAsO <sub>4</sub> SI	BaCrO <sub>4</sub> SI
1	1.29E-04	1.29E-04	4.18E-08	3.08E-03	2.19	-0.8	-1.6
2	1.29E-04	1.29E-04	1.32E-04	3.08E-03	2.19	-0.8	1.89
3	2.89E-04	2.89E-04	1.87E-08	1.38E-03	2.89	-0.799	-1.6
4	2.89E-04	2.89E-04	5.90E-05	1.38E-03	2.89	-0.799	1.89
5	5.78E-04	5.78E-04	9.33E-09	6.88E-04	3.49	-0.8	-1.6
6	5.78E-04	5.78E-04	2.95E-05	6.88E-04	3.49	-0.8	1.89

**Table 2.** Solution concentrations for experiments conducted at 1.0M NaCl with Barite saturation indices of 0.316, 1.02, and 1.62.

Experiment	BaCl <sub>2</sub> (M)	Na <sub>2</sub> SO <sub>4</sub> (M)	Na <sub>2</sub> CrO <sub>4</sub> (M)	Na <sub>2</sub> HAsO <sub>4</sub> (M)	BaSO <sub>4</sub> SI	BaHAsO <sub>4</sub> SI	BaCrO <sub>4</sub> SI
1	1.29E-04	1.29E-04	4.18E-08	3.08E-03	0.316	-3.00	-3.80
2	1.29E-04	1.29E-04	1.32E-04	3.08E-03	0.316	-3.00	-0.305
3	2.89E-04	2.89E-04	1.87E-08	1.38E-03	1.02	-3.00	-3.80
4	2.89E-04	2.89E-04	5.90E-05	1.38E-03	1.02	-3.00	-0.302
5	5.78E-04	5.78E-04	9.33E-09	6.88E-04	1.62	-3.00	-3.80
6	5.78E-04	5.78E-04	2.95E-05	6.88E-04	1.62	-3.00	-0.302

**Table 3.** Increased solution concentrations for experiments conducted at 1.0M NaCl with original Barite saturation indices of 2.19, 2.89 and 3.49.

Experiment	BaCl <sub>2</sub> (M)	Na <sub>2</sub> SO <sub>4</sub> (M)	Na <sub>2</sub> CrO <sub>4</sub> (M)	Na <sub>2</sub> HAsO <sub>4</sub> (M)	BaSO <sub>4</sub> SI	BaHAsO <sub>4</sub> SI	BaCrO <sub>4</sub> SI
1	1.11E-03	1.11E-03	7.77E-07	5.74E-02	2.19	-0.8	-1.60
2	1.11E-03	1.11E-03	2.40E-03	5.74E-02	2.19	-0.8	1.89
3	2.49E-03	2.49E-03	3.45E-07	2.55E-02	2.89	-0.8	-1.60
4	2.49E-03	2.49E-03	1.09E-03	2.55E-02	2.89	-0.8	1.89
5	4.98E-03	4.98E-03	1.73E-07	1.28E-02	3.49	-0.8	-1.60
6	4.98E-03	4.98E-03	5.47E-04	1.28E-02	3.49	-0.8	1.89

First, 1.0 M stock solutions of BaCl<sub>2</sub>, Na<sub>2</sub>HAsO<sub>4</sub>, Na<sub>2</sub>CrO<sub>4</sub>, NaCl and Na<sub>2</sub>SO<sub>4</sub> were prepared. The solutions of BaCl<sub>2</sub>, Na<sub>2</sub>HAsO<sub>4</sub>, and Na<sub>2</sub>CrO<sub>4</sub> were added to a 250mL beaker while a solution of Na<sub>2</sub>SO<sub>4</sub> was added to a 250mL beaker. For the specific experiments without the addition of NaCl, two more 250mL beakers were filled with 250mL of deionized water and combined into a 500mL beaker. For the experiments with the addition of NaCl, 250mL of NaCl was equally distributed between two beakers that were then filled with 250mL of deionized water.

A 5mL sample from each experiment was collected with 0.2 µm syringe filter before the initial mixing of solutions, after 30 minutes of reaction, and after 24 hours. The pH was also recorded before the initial mixing of the solutions as well as 24 hours after the initial mixing of the solutions. Na<sub>2</sub>SO<sub>4</sub> was added to simulated fracking wastewater which caused precipitated solids to form. Each 500mL solution was filtered in order to separate the solid particles from the aqueous phase of solution. The precipitated solids produced from the simulated wastewater treatment experiments were weighed after drying. Then, x-ray fluorescence was used to further analyze the solids for Chromium, Arsenic, and Barium present in the precipitated solids. XRF measurements were conducted in triplicate for each sample.

### X-Ray Fluorescence Calibrations and Analysis

The solids from simulated wastewater treatment experiments were examined using Niton XL2 X-ray Fluorescence (XRF) to measure for Chromium, Arsenic, and Barium. Data retrieved from the XRF was processed using PyMca5.5.5. computer software. Calibration curves were determined to accurately measure for Chromium, Arsenic, and Barium in solids produced from the experiments.

For the calibration of Chromium, pellets of polyacrylic acid (PAA) were mixed with Na<sub>2</sub>CrO<sub>4</sub>•7H<sub>2</sub>O. Pellets were mixed to have approximate concentrations of 446.92, 44.7, 4.9899, 31841, 167351, 78501.8, 16408, 8458.6, and 8211 ppm Chromium. The weighted amounts of polyacrylic acid (PAA) were mixed for 3 minutes using a mortar and pestle and pressed into a pellet with a hydraulic press. Similarly, pellets were prepared using Na<sub>2</sub>HAsO<sub>4</sub>, with concentrations of 1013.26, 506.63, 101.326, 50.663, and 5.0663 ppm Arsenic. For Barium, pellets were prepared with PAA and BaCl<sub>2</sub> to have concentrations of 1001.7, 500.85, 100.17, 50.085, and 5.0085 ppm Barium. The grams of Chromium, Arsenic, or Barium was calculated using the following equation:

$$\begin{aligned}
& 10 \text{ mg (Cr, As, or Ba)} \times \frac{1 \text{ g}}{1000 \text{ mg}} \times \text{molar mass (Cr, As, or Ba)} \\
& \times \frac{1 \text{ mol (Na}_2\text{CrO}_4 \cdot 7\text{H}_2\text{O, Na}_2\text{HAsO}_4, \text{ or BaCl)}}{1 \text{ mol (Cr, As, or Ba)}} \\
& \times \frac{(\text{molar mass of Na}_2\text{CrO}_4 \cdot 7\text{H}_2\text{O, Na}_2\text{HAsO}_4, \text{ or BaCl)}}{1 \text{ mol (Na}_2\text{CrO}_4 \cdot 7\text{H}_2\text{O, Na}_2\text{HAsO}_4, \text{ or BaCl)}} \\
& = \text{Amount of Na}_2\text{CrO}_4 \cdot 7\text{H}_2\text{O, Na}_2\text{HAsO}_4, \text{ or BaCl (g) Used}
\end{aligned}$$

The initial mixtures of both PAA and Na<sub>2</sub>CrO<sub>4</sub>•7H<sub>2</sub>O, Na<sub>2</sub>HAsO<sub>4</sub>, or BaCl<sub>2</sub> were diluted with more PAA to reach concentrations of Chromium, Arsenic, and Barium. Each pellet was analyzed using X-ray Fluorescence (XRF) for 60 seconds under plastic wrap. The XRF data collected was processed using PyMca5.5.5 to determine the fit areas in the spectra for Chromium, Arsenic and Barium fluorescence in all samples. For our calibration curves, the fit areas were plotted against the respective known concentrations of Chromium, Arsenic, and Barium, and a linear regression was used to relate Chromium, Arsenic, and Barium concentration to fit area (Fig. 1 – 3). The first pellet ppm concentration was calculated using the following equation:

$$\frac{\text{mass of Cr, As, or Ba (mg)}}{\text{mass of PAA (kg)}} = \text{ppm}$$

The rest of the pellets, following the ppm calculation for the first pellet, were calculated using a C<sub>1</sub>V<sub>1</sub> = C<sub>2</sub>V<sub>2</sub> equation. The equation is as follows:

$$\begin{aligned}
& (\text{the exact mass of Na}_2\text{CrO}_4 \cdot 7\text{H}_2\text{O, Na}_2\text{HAsO}_4, \text{ or BaCl} \\
& \quad + \text{added mass of previous pellet})(\text{previous pellet's ppm}) \\
& = (C_2)(\text{exact mass of PAA})
\end{aligned}$$

$$(C_2) = \text{calculated concentration (ppm)} \quad \text{*solve for } C_2$$

The XRF data from the simulated wastewater treatment experiments were similarly processed using PyMca5.5.5. to determine the fit areas for Chromium, Arsenic, and Barium in the spectra. Because samples were analyzed in triplicate, the fit areas from the 3 measurements were averaged. The Chromium, Arsenic, and Barium concentrations were calculated from fit areas using the equations for the linear regressions from Fig. 1 – 3.

The Chromium, Arsenic, and Barium concentrations were then converted to moles using the final masses collected of collected solids for each experiment in Table 4, 5, and 6 using the following equation:

$$\begin{aligned}
& \frac{\text{mg (Cr, As, or Ba)}}{\text{kg total solid}} \times \frac{1 \text{ g (Cr, As, or Ba)}}{1000 \text{ mg}} \times \text{molar mass of element (Cr, As, or Ba)} \\
& \quad \times \text{total mass} \\
& = \text{Cr, As, or Ba (mol)}
\end{aligned}$$

The measurements of Chromium, Arsenic, and Barium in moles were used to calculate Arsenic/Barium and Chromium/Barium molar ratios.

**Results**

**Table 4 – 6.** Final masses of precipitated solids collected for Experiments 1 to 6 for No NaCl, NaCl, and NaCl with new activity.

Table 4		Table 5		Table 6	
No NaCl		NaCl		NaCl with New Activity	
Experiment	Mass of Final Product (g)	Experiment	Mass of Final Product (g)	Experiment	Mass of Final Product (g)
1	0.005	1	0.013	1	0.279
2	0.005	2	0.0022	2	0.149
3	0.003	3	0.014	3	0.274
4	0.009	4	0.015	4	0.346
5	0.022	5	0.007	5	0.37
6	0.026	6	0.004	6	0.373

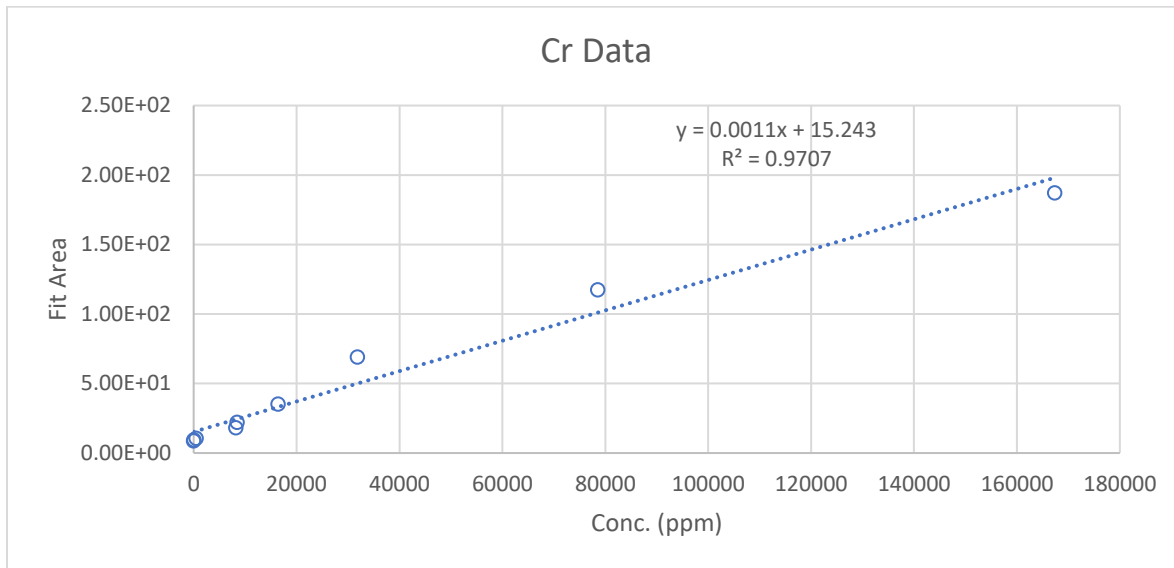


**Figure 1.** Cr concentrations (ppm) vs. Fit Area from PAA experiments.



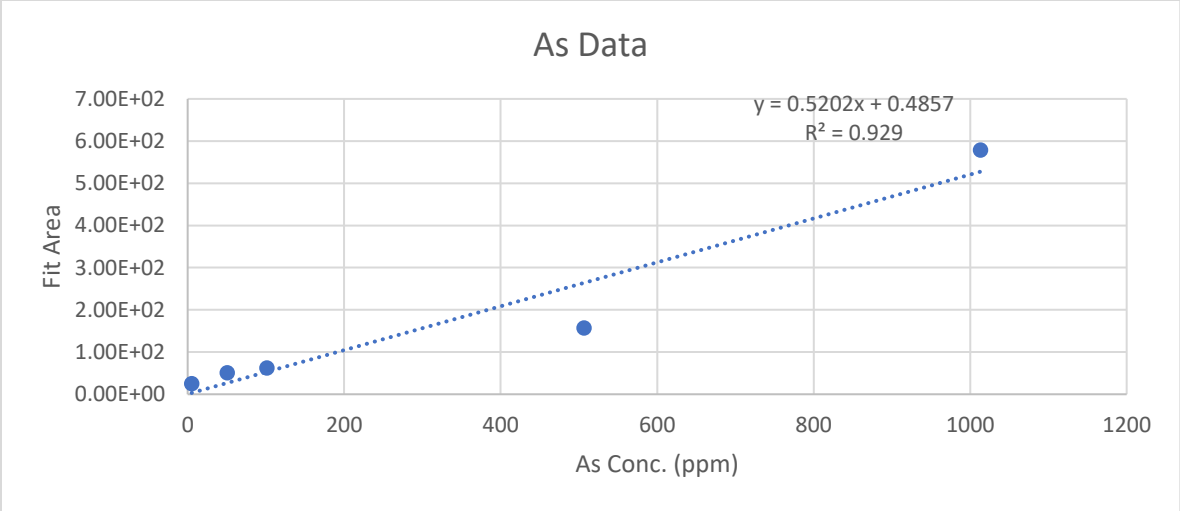


Figure 2. As concentrations (ppm) vs. Fit Area from PAA experiments.

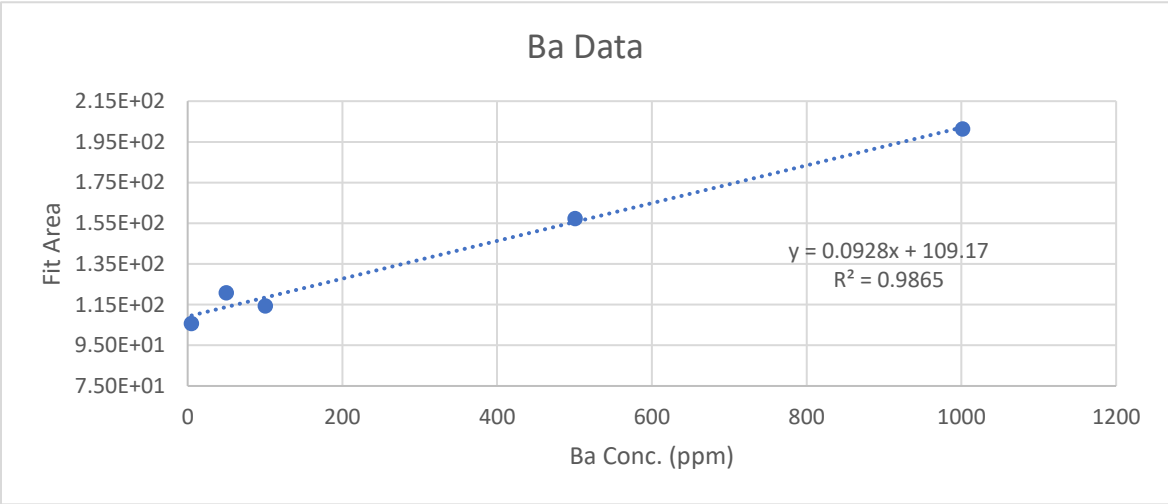
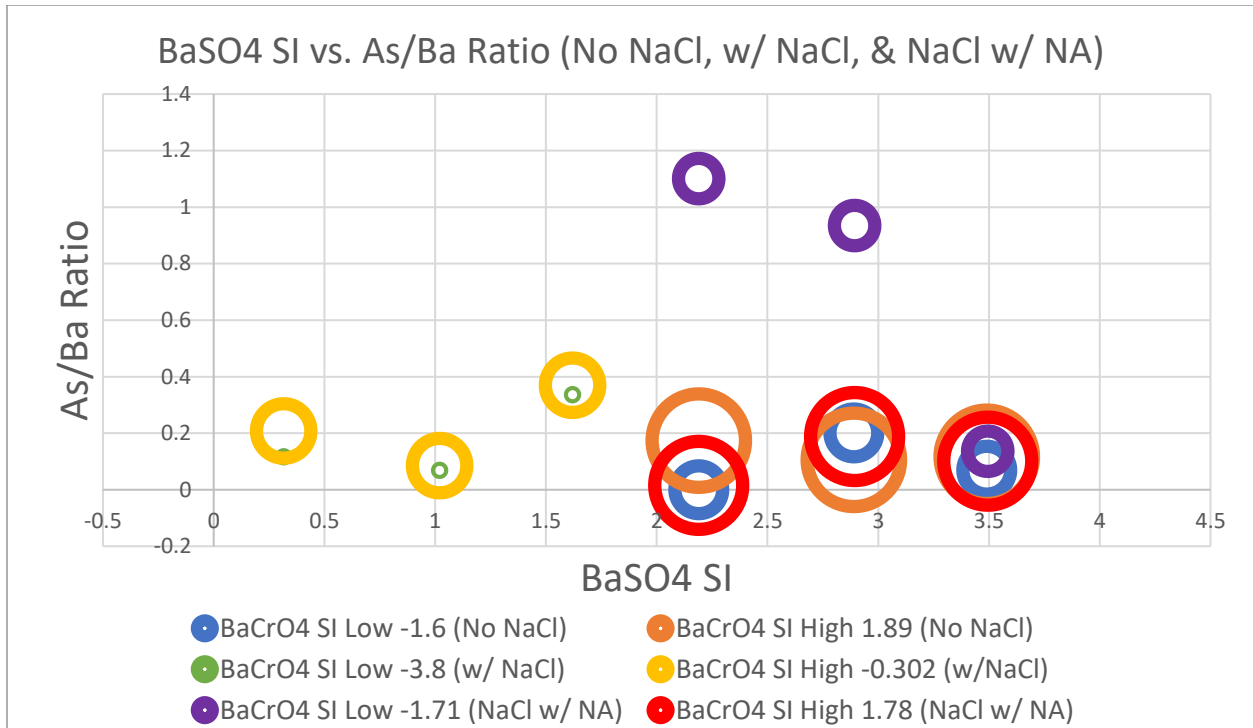
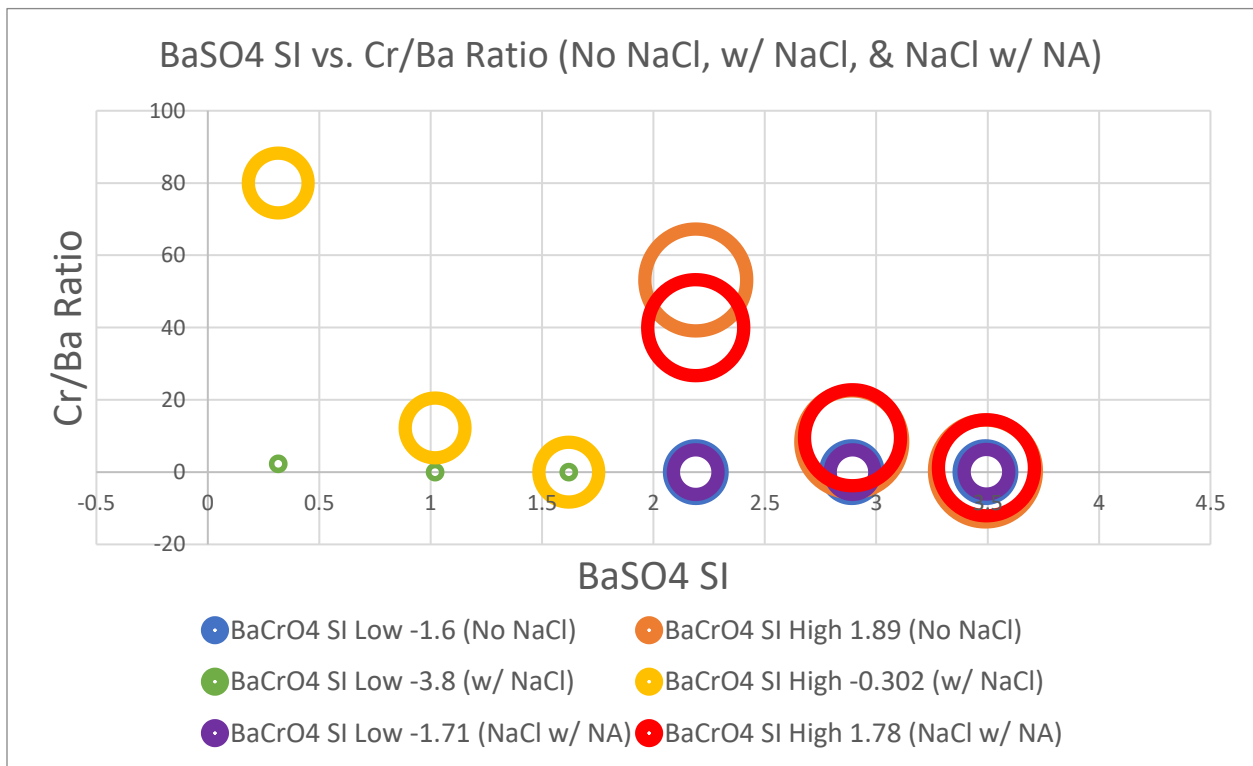


Figure 3. Ba concentrations (ppm) vs. Fit Area from PAA experiments.



**Figure 4.** BaSO<sub>4</sub> saturation index (SI) vs. Arsenic/Barium ratio (mol) with NaCl, without NaCl, and with new activity of NaCl.



**Figure 5.** BaSO<sub>4</sub> saturation index (SI) vs. Chromium/Barium ratio (mol) with NaCl, without NaCl, and with new activity of NaCl.

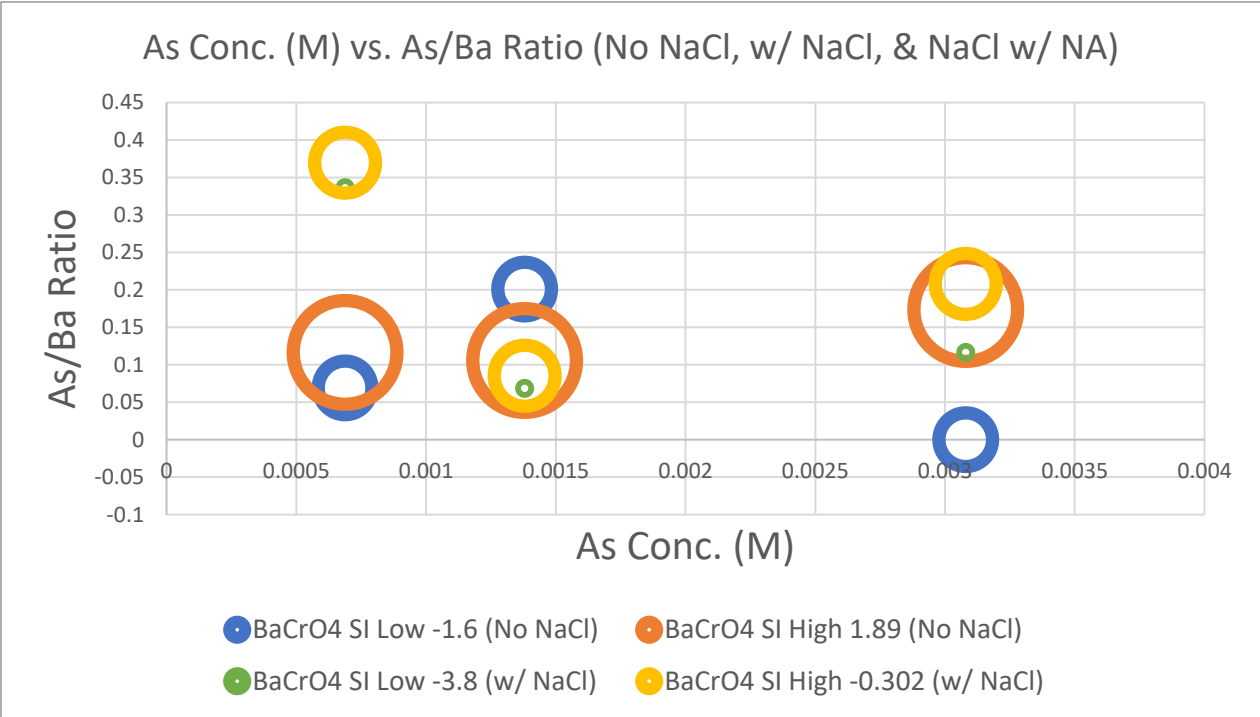
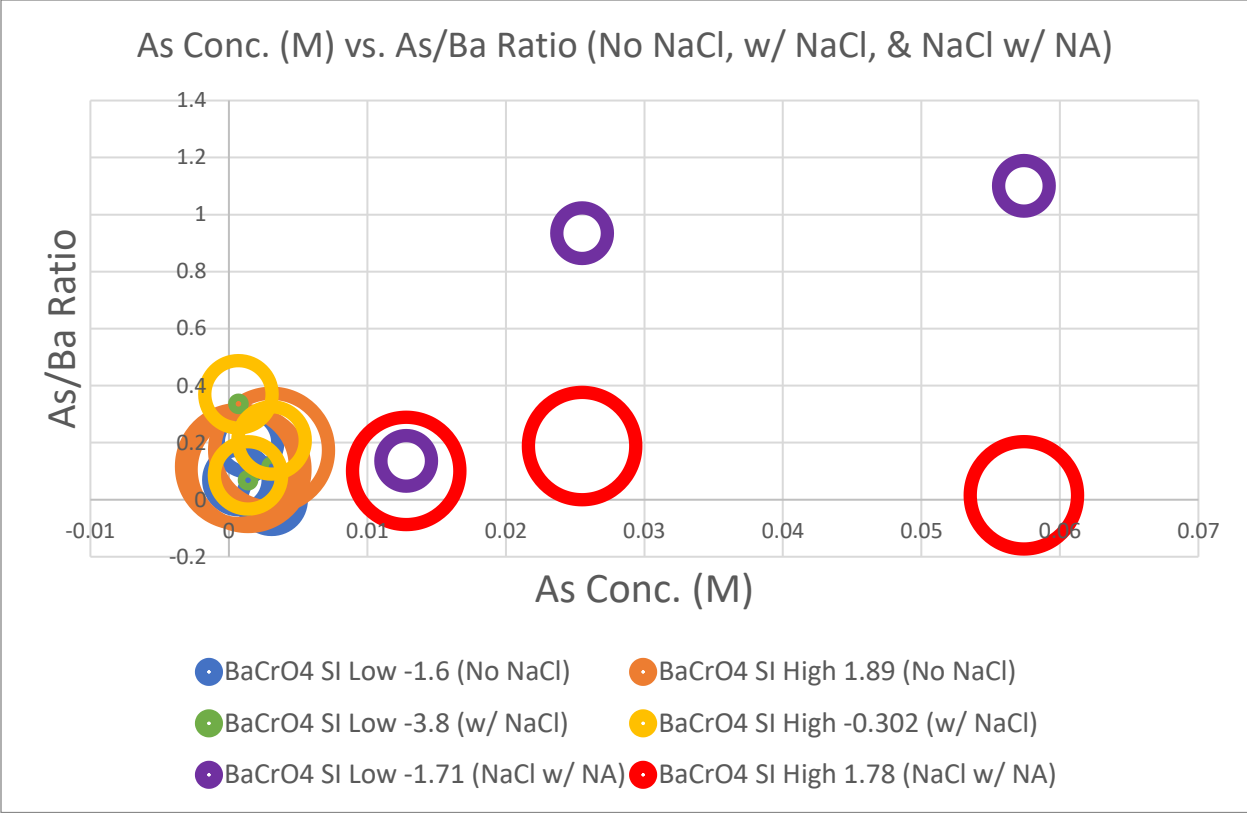


**Figure 6a-6b.** Arsenic concentration (M) vs. Arsenic/Barium ratio (mol) with NaCl, without NaCl, and with new activity of NaCl. Figure 6b excludes new activity of NaCl.

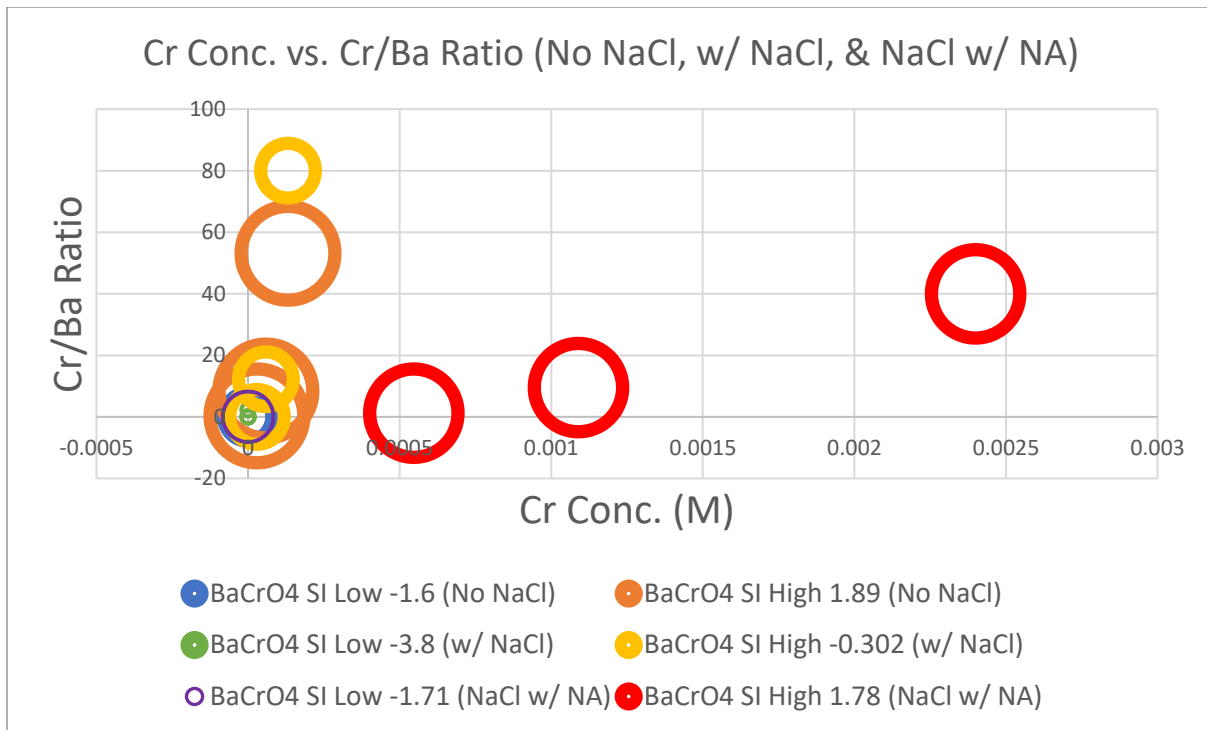


**Figure 7.** Chromium concentration (M) vs. Chromium/Barium ratio (mol) with NaCl, without NaCl, and with new activity of NaCl.

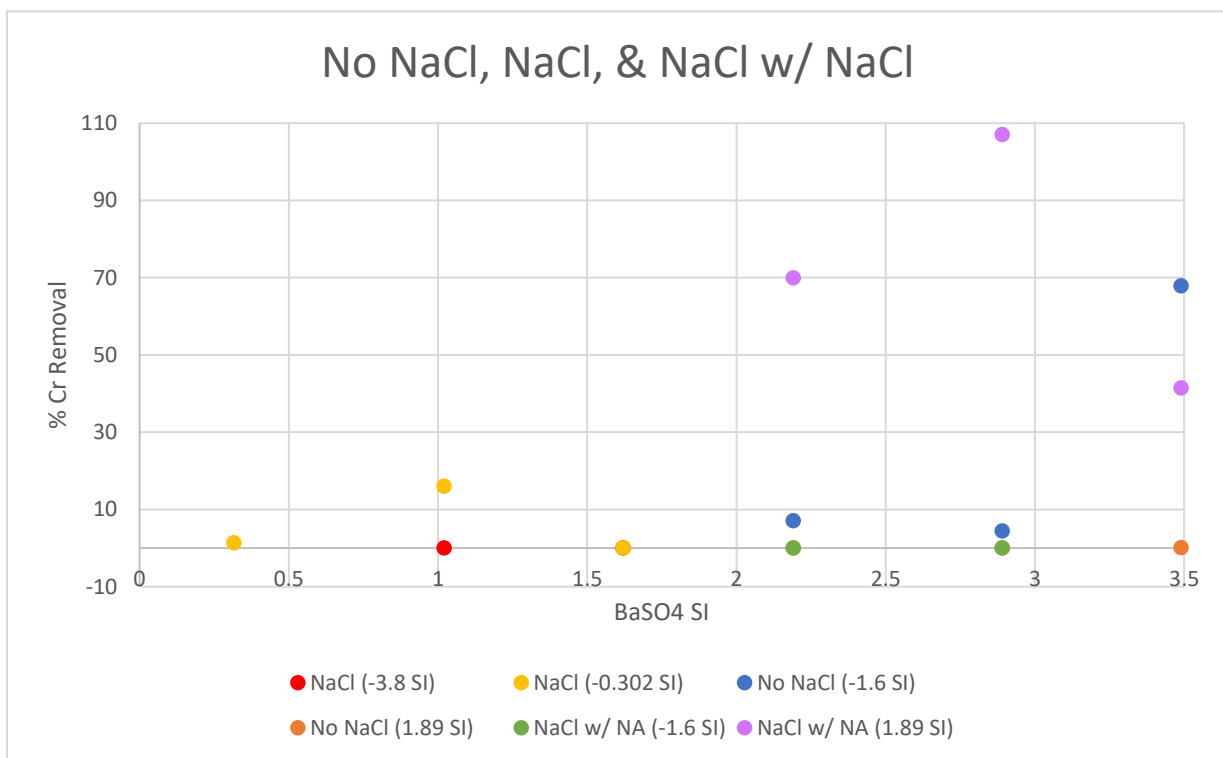


**Figure 8.** BaSO<sub>4</sub> saturation index (SI) vs. percentage of Chromium removal with NaCl, without NaCl, and with new activity of NaCl.

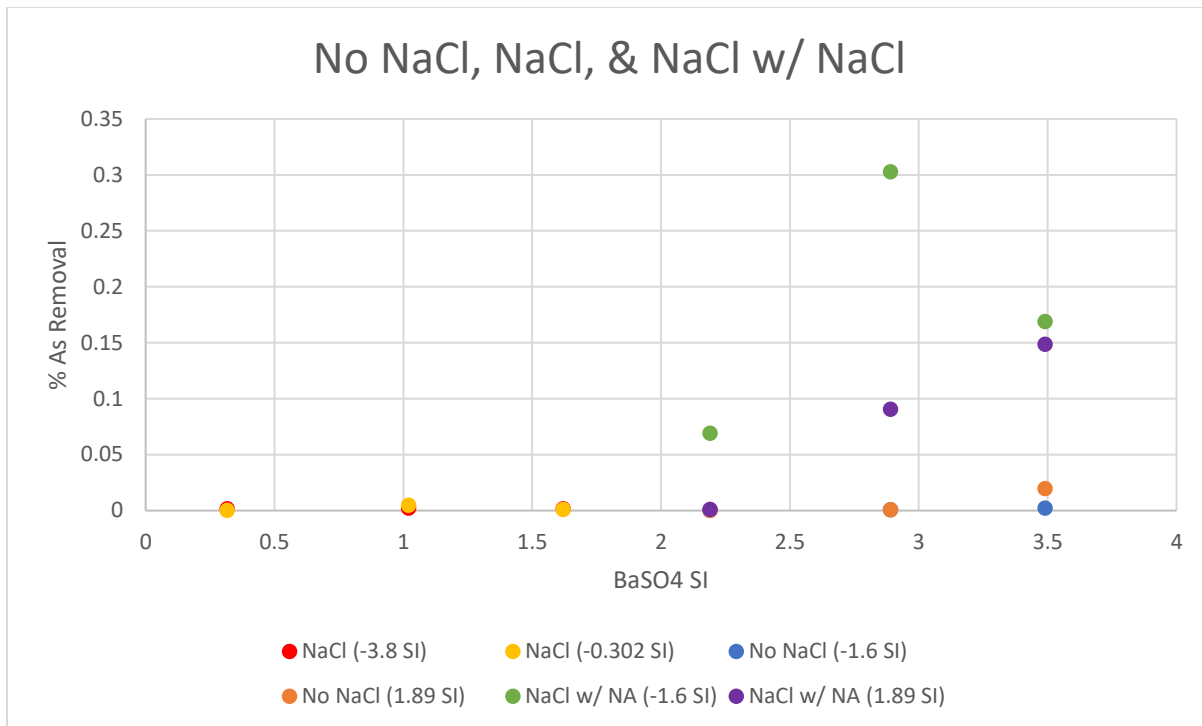


**Figure 9.** BaSO<sub>4</sub> saturation index (SI) vs. percentage of Arsenic removal with NaCl, without NaCl, and with new activity of NaCl.

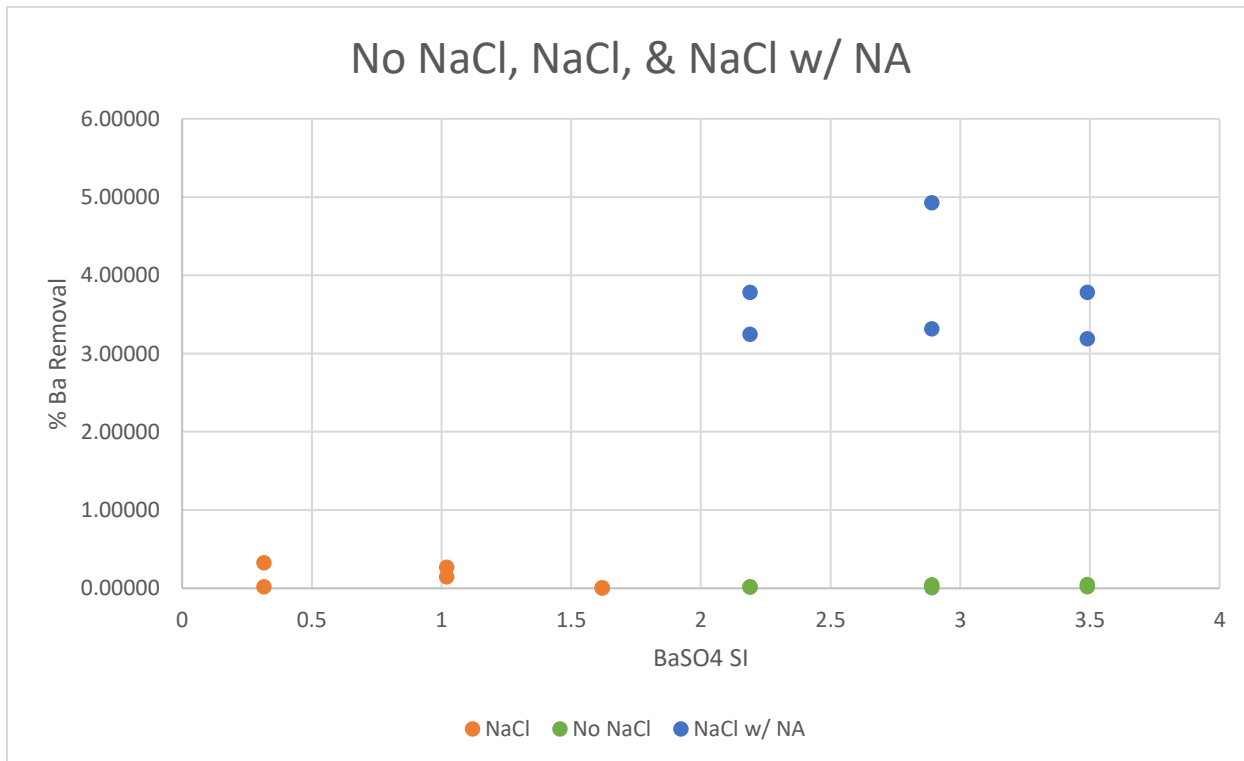


**Figure 10.** BaSO<sub>4</sub> saturation index (SI) vs. percentage of Barium removal with NaCl, without NaCl, and with new activity of NaCl.

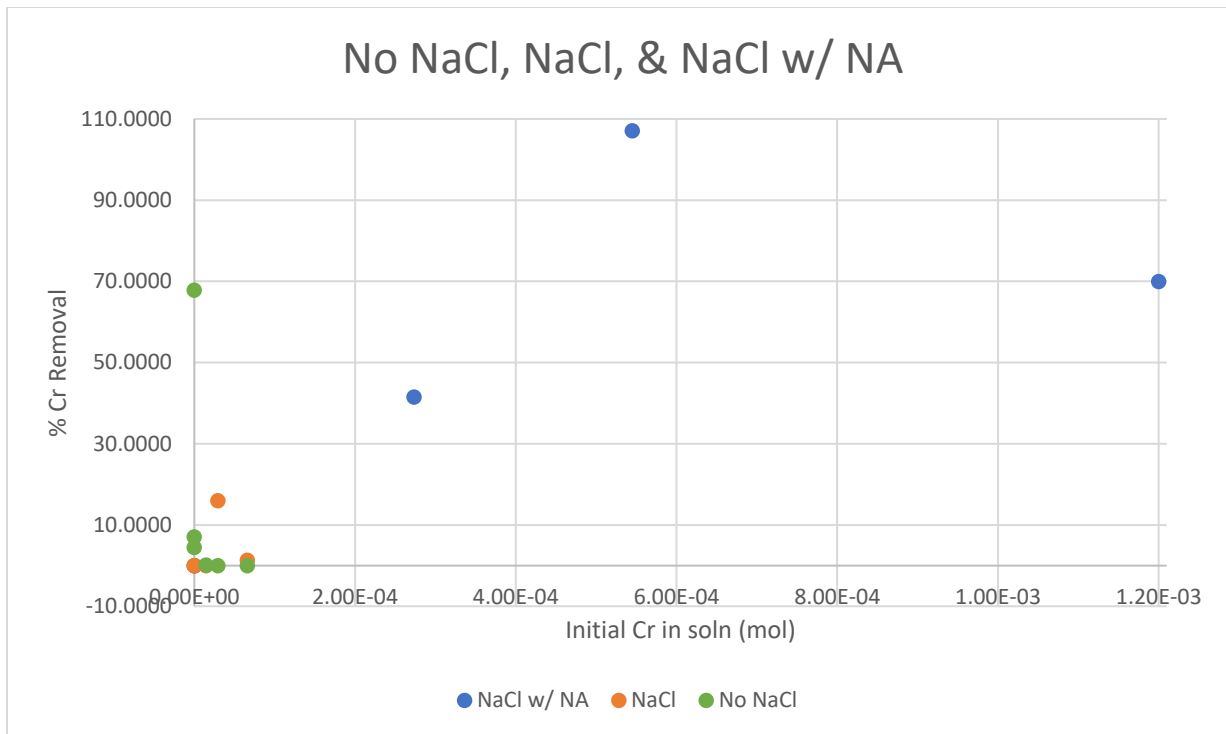


**Figure 11.** Initial Chromium in solution. (mol) vs. percentage of Barium removal with NaCl, without NaCl, and with new activity of NaCl.

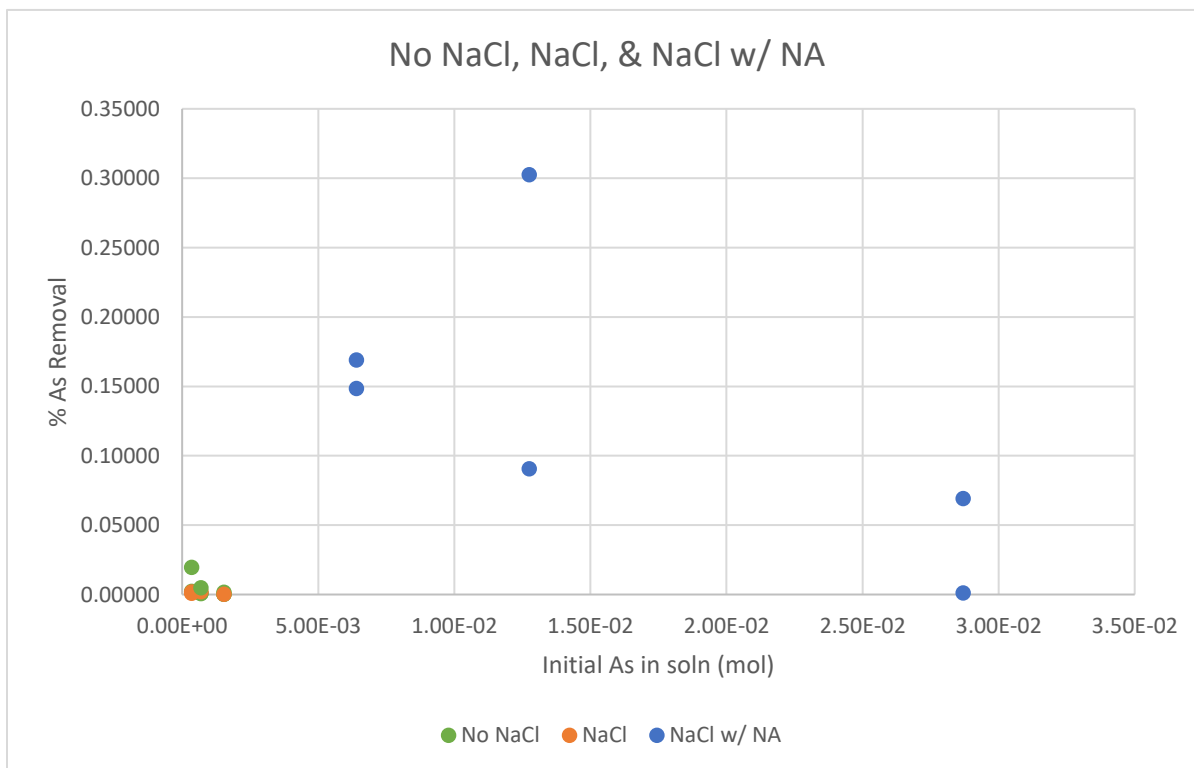


**Figure 12.** Initial Arsenic in solution (mol) vs. percentage of Barium removal with NaCl, without NaCl, and with new activity of NaCl.

## **Discussion:**

### **Chromium Removal**

In Figure 5, as the  $\text{BaSO}_4$  SI increases, the Chromium/Barium ratio (mol) is decreasing. When the Barium Chromate indices are low, the Chromium/Barium mol ratio is near or equal to 0 indicating that Chromium removal is very low. In Figure 7, as Chromium concentration increases, the Chromium/Barium mol ratio increases.

### **Arsenic Removal**

In Figure 4, there is no clear correlation between the saturation index of  $\text{BaSO}_4$  and the ratio of Arsenic/Barium (mol). When the  $\text{BaSO}_4$  saturation index is less than 2, the Arsenic/Barium mol ratio generally increases with  $\text{BaSO}_4$  saturation index. When the  $\text{BaSO}_4$  saturation index is greater than 2, the Arsenic/Barium mol ratio decreases with increasing  $\text{BaSO}_4$  saturation index when Barium Chromate saturation index is low. When the  $\text{BaSO}_4$  saturation index is greater than 2 and the Barium Chromate saturation index is greater than -1.6, the Arsenic/Barium mol ratio remains low. This is likely because at higher Barium Chromate saturation indices, Chromium outcompetes Arsenic for bonding sites in Barite.

In Figure 6, at Arsenic concentrations greater than 0.01 M, the Arsenic/Barium mol ratio generally increases. When the Arsenic concentration (M) is less than 0.01 M, the Arsenic/Barium mol ratio generally decreases when Barium Chromate saturation index is low. When the Arsenic concentration (M) is less than 0.01 M, the Arsenic/Barium mol ratio generally increases when Barium Chromate saturation index is high. This is likely because as Arsenic concentration increases, there is more of a chance for Arsenic to bond in Barite while competing with Chromium.

### **Effect of Salinity**

There is not much of a distinguishable difference between the masses of the solids with and without added NaCl. Masses of experiments 1, 3, and 4 are slightly heavier with NaCl added while experiments 2, 5, and 6 are slightly lighter with NaCl added. The masses for NaCl with new activity are all significantly heavier than solids with and without NaCl added. (Refer to Table 4 – 6).

Salinity, specifically NaCl with new activity, causes high percentage removal of Chromium, Arsenic, and Barium. In Figures 8 – 10, salinities are compared using  $\text{BaSO}_4$  saturation index plotted against percentage of removal. Each figure shows NaCl with new activity has significantly higher removal percentages compared to No NaCl and NaCl. For Chromium percentage removal, Figure 8, No NaCl with a high saturation index shows a high percentage; the reason for this is yet to be determined.

High percentage of removal is also impacted by salinity when being plotted against the initial measurements of Chromium and Arsenic in solution (mol). In Figures 11 and 12, NaCl with new activity shows a significantly higher percentage of removal results compared to No NaCl and NaCl. When there is salinity, removal percentages increase significantly.

## Implications

Researching ways to remove hazardous toxins from fracking wastewater is both beneficial to the environment and to human health. Fracking has become popularized in recent years and will only grow in popularity. It is important that research on environmental topics like fracking wastewater treatments be explored because, as mentioned in previous studies, the topic has not been researched to the degree as other popular environmental concerns. With the help of more research and funding, a true difference can be seen in the impacts of hazardous ions in fracking wastewater that can negatively impact human and environment health. Future work with this particular research could include working on expanding the supply of treatment, finding easier ways of transporting and distributing such treatment, and more in-depth research on various other treatment options.

## References

1. Lutz, BD., Lewis, AN., Doyle, MW. Generation, transport, and disposal of wastewater associated with Marcellus Shale gas development. *Water Resource*. 2013, **49**, 647-56.
2. Denchak, Melissa. "Fracking 101." *NRDC*, Natural Resources Defense Council 2019, 19 April 2019.
3. Bamberger, M., & Oswald, R. E. (2012). Impacts of Gas Drilling on Human and Animal Health. *NEW SOLUTIONS: A Journal of Environmental and Occupational Health Policy*, 22(1), 51-77. doi:10.2190/ns.22.1.e
4. Hammer, R., VanBriesen, J., & Levine, L. (2012). In fracking's wake: new rules are needed to protect our health and environment from contaminated wastewater. *Natural Resources Defense Council*, 11.
5. Tchounwou, Paul B et al. "Heavy metal toxicity and the environment." *Experientia supplementum* (2012) vol. 101 (2012): 133-64. doi:10.1007/978-3-7643-8340-4\_6
6. Goodin, Mitchell. "Deep Well Injections." *Geoengineer*, Elxis S.A., 20 November 2017.
7. Zhang, T., Gregory, K., Hammack, R., Vidic, R. Co-precipitation of Radium with Barium and Strontium Sulfate and Its Impact on the Fate of Radium during Treatment of Produced Water from Unconventional Gas Extraction. *Environ. Sci. Technol.* 2014, **48**, 4596-4603.
8. Shaffer, D. L., Arias Chavez, L. H., Ben-Sasson, M., Romero-Vargas Castrillón, S., Yip, N. Y., & Elimelech, M. (2013). Desalination and reuse of high-salinity shale gas produced water: drivers, technologies, and future directions. *Environmental science & technology*, 47(17), 9569-9583.
9. Erikson, Britt E. "Wastewater from Fracking: Growing Disposal Challenge or Untapped Resource?" *Chemical & Engineering News*, American Chemistry Society, 17 November 2019.



10. Ling, F.T., Hunter, H.A., Fitts, J.P. *et al.* Nanospectroscopy Captures Nanoscale Compositional Zonation in Barite Solid Solutions. *Sci Rep* **8**, 13041 (2018).
11. Tokunaga, K., & Yoshio Takahashi. Effective Removal of Selenite Ions from Aqueous Solution by Barite (2017). *Environmental Science & Technology*, *51* (16), 9194-9201.
12. L'Heureux, I. & Jamtveit, B. A model of oscillatory zoning in solid solutions grown from aqueous solutions: Applications to the (Ba, Sr) SO<sub>4</sub> system. *Geochim. Cosmochim. Acta* *66*, 417–429 (2002).
13. Breit, G. N., Simmons, E. C., & Goldhaber, M. B. (1985). Dissolution of barite for the analysis of strontium isotopes and other chemical and isotopic variations using aqueous sodium carbonate. *Chemical Geology: Isotope Geoscience section*, *52*(3-4), 333-336.
14. Noguera, C., Fritz, B., Clément, A. & Amal, Y. Simulation of the nucleation and growth of binary solid solutions in aqueous solutions. *Chem. Geol.* *269*, 89–99 (2010).